Egypt. J. Chem. **Vol. 66**, No. 2 pp. 267 - 281 (2023)

Egyptian Journal of Chemistry

http://ejchem.journals.ekb.eg/

Characterization, Antimicrobial and Antitumor Investigation for Substituted Cyclodiphosph (V) azane sulfa medicines and their Transition Metal Complexes.

Salwa A.H.Albohy,[a*] Rania H. Taha,[a,b] Carmen M. Sharaby,[a*]

[a] *Chemistry Department, Faculty of Science(Girls), Al-Azhar University, Nasr City, Cairo,P.O: 11754 Egypt,* [b] *College of Science, Jouf University, , Sakaka, Saudi Arabia Postal code:. Box: 2014.*

Abstract

A ligand of geminal cyclodiphosph(V)azane derivatives, 1,3-di-[N-2,6-dimethoxy-4-pyrimidnylsulfanilamide]-2-sulfanilamidopyrimidine]-2,4-dichlorocyclo-diphosph(V)azane(H_4L) was prepared. The ligand was reacted with several transition metals such as ferric (III), manganese (II), cobalt (II), copper (II), zinc (II) and cadmium (II) chlorides and uranium (II) nitrate in a 1:2; L: M mole ratio to produce colorful complexes in a good yield. Diffraction investigations approaches were used to analyze the ligand and its transition metal complexes, including elemental composition and UV-vis, infrared spectra (IR), 1H NMR, magnetic susceptibility, molar conductance, solid reflectance, thermal analysis, and X-ray powder diffraction investigations. The ligand has an ionic character and coordinates with the metal ions via enolic OH of the sulphonamide group and pyrimidine–N according to the spectrum data. Data on molar conductance reveals that the complexes were electrolytes, according to UV-vis, magnetic moment, and solid reflectance. It has been shown that the complexes have octahedral geometry. The antibacterial activity of the ligand as well as its metal complexes ranged from high to medium against different fungi as well as strains of bacteria, and also demonstrated an anticancer effect against colon carcinoma HCT116.

Keywords: sulfa drugs; cyclodiphosph(V)azane derivatives; colon carcinoma; standard cancer cell lines.

1. Introduction

In the periodic table of elements, no congeners create more structurally diverse compounds than nitrogen and phosphorus [1]. Single, double, and triple bonds can be formed by these nonmetals. It was also because of the strength of the P–N bonds, which make most phosphorus–nitrogen compounds extremely thermally stable [2]. The P–Cl connection, as well as the relative geometry of phosphorus substituents, have been the subject of much of the previous research [1, 2]. Other researchers discussed the compounds' potential as very flexible ligands and macrocyclic precursors in subsequent years [3, 4]. Utility of these compounds for a number of industrial and chemical applications as flame retardants sparked [5]. Sulfonamide complex compounds are frequently employed as anti-inflammatory, antifungal, and hypoglycemic medications. Sulfonamide base ligands' pharmacology and toxicity can be altered by metal complexes. The ability of sulfonamide cyclodiphosphazanes to form more physiologically active complexes has been explored [6–8]. Sulfonamide is a generic name for derivatives of para-aminobenzene sulfonamide which possess enormous efficient bioactivities such as antiangiogenic [7,8], antitumor [9], anti-inflammatory and anti-analgestic [10]. Sulphonamides belong to the group of antibacterial drugs, which are used for human and animal therapy, to cure infectious diseases of digestive and respiratory systems, affections of the skin (in the form of ointments) and for prevention or therapy of coccidiosis of small domestic animals [11,12]. Quality control of sulphonamide formulations and their quick systematic monitoring in body fluids are important analytical tasks. A number of articles have been published concerning the determination of sulphonamides by different analytical methods. Sulfamerazine is one of the well-known and widely used sulfonamide antibacterial drugs to treat bacterial disease in human and animals like cattle, sheep, pigs and poultry [11,12]. Transition metal complexes are

*Corresponding author e-mail: salwaalbohy.59@azhar.edu.eg

Receive Date: 28 April 2022, Revise Date: 13 May 2022, Accept Date: 18 May 2022

DOI: 10.21608/EJCHEM.2022.136363.6007

quite well known for their ability to speed up a therapeutic agent's action and efficiency. Complexation has proven to be a beneficial strategy for increasing the biological activities of ligands. A medicinal agent's action and efficiency can often be improved by coordinating with a metal ion. The current work seeks to construct substituted hexachlorocyclodiphosph(V)azane of sulfadimethoxine H2L in continuation of our interest in preparing hexachlorocyclodiphosph(V)azane of sulfa medicines. The interaction of these ligands with transition metal ions was studied. A number of physicochemical approaches were used to characterize the produced compounds. The synthesized ligands and their complexes were also tested for biological and anticancer activities.

2. Experimental:

2.1. Reagents

Aldrich or BDH provided all of the chemicals. They were purified when required. Standard techniques were used to purify the solvents [10].

2.2. Synthesis of 1,3-di-[N-2,6-dimethoxy-4-pyrimidnylsulfanilamide]-2,4-di-2-sulfanila-midopyrimidine]-2,4-dichlorocyclodiphosph(V)azane (H_4L) ligand.

1,3-di-[N-2,6-dimethoxy-4-primidnylsulfanilamide]-2,2,2,4,4,4-hexachlorocyclodipho- sph(V)azane (H2L) was synthesized in previous work [11] and used by Chapman et al. [12] and Kirzanov and Zhumurova [13] by condensation of pcl_5 and sulfamethoxazole in dry benzene for 3hrs. During half an hour, small amounts of mono silver sulfadiazine [mono silver-2-sulfanilamidopyrimidine] (7.143 g, 0.02 mole) were introduced to a well stirred cold solution of H_2L (8.056 g, 0.01mol) in 100 ml of acetonitrile in a quick fit flask. After completion of the addition, reflux was applied to the reaction mixtures for three hours. As shown in scheme 1, filtration was used to separate the solid products, which were then refined by washing with acetonitrile, diethyl ether, and vacuum drying over anhydrous $CaCl_2$ to provide the corresponding substituted cyclodiphosphazane of sulfa drug H_4L.

2.3. Synthesis of the complexes

At room temperature, a solution of metal salts of ferric, manganese, cobalt, copper, zinc and cadmium chloride and uranium nitrate respectively (10 mmol) in 50 ml dry well-stirred ethanol was dropped into an H_4L ligand -based solution (5 mmol) in 100 ml dry ethanol. The reaction mixture was heated under reflux for two hours, the temperature of the reaction mixture was kept constant. The products were separated and washed in ethanol and diethyl ether numerous times before being vacuum dried. Produce metal complexes from (1-7) Table 1 summarizes the information data for complexes.

2.4. Instrumentation

At Cairo University's Microanalytical Center, microanalytical determinations (C, H, N, S, and P) were made. The infrared spectrum was recorded using a Perkin–Elmer spectrometer. Model 437 infrared spectrophotometer (400–4000cm-1) (KBr technique). A Pruker FT-400MHZ spectrophotometer was used to measure 1H NMR spectra (DMSO-d6) without employing an internal standard. A Shimadzu PC 3101 spectrophotometer was used to measure the electronic spectra. On a Sherwood Scientific Magnetic Susceptibility Balance, the magnetic susceptibilities of the solid-state complexes have been measured using the Faraday technique. In a nitrogen environment, on a Shimadzu-50H, thermal gravimetric measurements (TGA) have been recorded. utilized thermal analyzer. A Perkin-Elmer Lambda 3B Ultraviolet–vis spectrophotometer was used to measure the UV–vis spectra. Mass spectra were recorded using a direct insertion probe (DIP) on a Shimadzu-Ge-Ms-QP 100 EX mass spectrometer (Japan) at temperatures ranging from 50 to 800 degrees Celsius. At room temperature, an Empress X-ray diffractometer was used to record X-ray diffraction (25oC). The device was operated at 45 KV and 30 mA, with a Cu target (CuK radiation). Using normal EDTA titration, the metal concentration was calculated complexometerically [14]. The phosphorus level was measured using phosphoammonium molybdate gravimetrically [15]. Antimicrobial activity was investigated using DMF as a solvent at the Fermentation Biotechnology and Applied Microbiology (FERM-BAM) Center. The diffusion agar technique was used to carry out the experiment. [16]. At Cairo University's National Cancer Institute, Cancer Biology Department, the compounds' potential cytotoxicity was assessed on the HCT116 cell line using the method of Skehan et al. (1990) [17].

3. Results and discussion

3.1. Characterization of the ligand

Hexachlorocyclodiphosph(V)azane derivative of 1,3-di-[N-2,6-dimethoxy-4-pyrimidnylsulfanilamide]-2,4-di-2-sulfanilamidopyrimidine]-2,4-dichlorocyclodiphosph(V)azane (H_4L) was synthesized. As shown in scheme 1, the analytical findings show the structure of the prepared ligand (H_4L). The cyclodiphosphazane free ligand was subjected to elemental analysis. The results of elemental analysis were shown in Table 1, together with molecular formulae and melting points. The results obtained were quite comparable to those obtained using the proposed formula. The melting temperatures of the produced ligand were extremely high, suggesting its purity. In the UV-vis spectra of the free ligand in (103-M) DMF as a solvent, the absorption band at 268 nm displays electron delocalization inside the dimeric structure of the ligand's phosphazo four-membered ring [18-19]. In addition, the ligand spectra show another absorption peak at 300 nm, which is indicative of the π-π* transition [20]. When one Cl atom was replaced by one molecule of sulfa medications in both locations of the dimeric structure of the ligand H4L, the band was moved to a lower wavelength (max = 270 nm) in comparison to the original ligand H_2L. Table 4

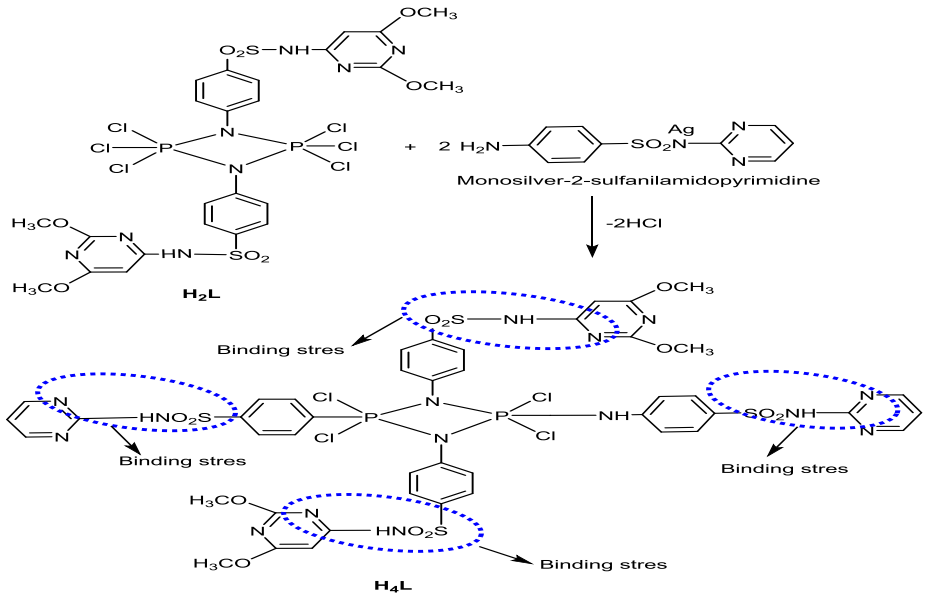

Scheme 1 Synthesis of 1,3-di-[N/-2,6-dimethoxy-4-pyrimidnylsulfanilamide] 2,4-di-2-sulfanila-midopyrimidine]2,4dichlorocyclodiphosph(V)azane (H_4L) free ligand.

The H_4L free ligand's ^1H NMR spectra in DMSO-d6 shows a broad signal. This ligand's SO_2NH appears at = 3.80–5.60 ppm, indicating that a silver ion of the silver sulfadiazine is replaced by a H atom during the substitution reaction. Furthermore, aromatic proton signals in their expected locations doubled by roughly 6.91- 7.66 ppm for H_4L [21,22]. The signal, which may be observed at 3.53 ppm, is created by OCH_3 protons. According to estimates, heterocyclic protons can be found at 8.64, 7.02, and 8.51 ppm [6] as shown in Fig.1.

The structure of the free ligand of the substituted cyclodiphosph(V) azane sulfa medicines was also validated by IR spectra. The stretching vibration bands characteristic of (P–N) were visible in the unbound ligand's IR spectra at 1153 cm^{-1} [23]. The ligand also has two bands at 1090 and 1321 cm^{-1}, which are ascribed to the sym.SO_2 and asym.SO_2 stretching vibrations alternately. At 3422 cm^{-1}, there are bands that are characteristic of an NH ligand for H_4L. In addition, the ligand spectrum revealed a novel band at 1585 cm^{-1}, which is caused by (C=N) diazine ring vibrational bands [24]. Furthermore, when one Cl atom was replaced by one molecule of each sulfa drug in both positions of the dimeric structure of the ligand, the 572cm^{-1} band due to (PCl) for the original ligand, H_2L, was moved to 555 cm^{-1} as shown in Fig. 2 and table 2.

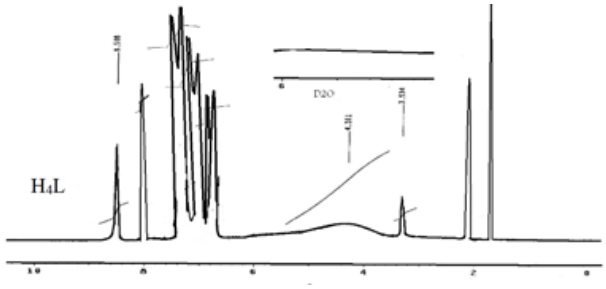

Fig.1. ^1H NMR spectrum of H_4L

3.2. Composition and structures of Metal complexes

The results of the elemental analyses of the isolated complexes Fe (III), Mn (II), Co (II), Cu (II), Cd (II), Zn (II) and UO_2 (II) ions (1−7) are in good agreement with those required by the proposed formula of complexes according to the following general equations:

$$2MXz+H_4L+nH_2O \rightarrow [(M)_2(H_4L)Cl_y(H_2O)_n]X_z$$

Where, M = Fe (III), Mn (II), Co (II), Cu (II), Cd (II), Zn (II) and UO_2(II) ions

Fe (III) (z = 2, X = Cl, y = 4, n = 0),

Mn (II), Co (II), Cu (II), Cd (II) and Zn (II) (z = 2, X = Cl, n = 2, y = 2),

UO_2(II) (z = 4, X = NO_3, y = n = 0).

The elemental analyses of these separate complexes are depicted in tables 1.

3.3. Molar conductance

Using the equation m = K/C, where C is the molar concentration of the metal complex solutions and K is the specific conductance, the conductivity value of the complexes (1–7) may be derived. At 25°C, the molar conductivities of the complex's solutions were measured after they were dissolved in (10^{-3}M) DMF. Table 1 displays the molar conductance values of H_4L and its transition metals complex (1–7) which exhibits molar conductance values in the range of 194.90–208.10 ohm^{-1}cm^2 mol^{-1}. According to results, these compounds are ionic in nature and belong to the 2:1 electrolyte type [25, 26]. The UO_2(II) (7) H_4L ligand complexes was the exception, with a molar conductance of 398.90 ohm^{-1} cm^{2}mol^{-1}. These findings indicate that these chelates should be classified as a 4:1 electrolyte. showing that the nitrate group's connection to the cationic complex is ionic [27].

Table1.Some physical measurements and Elemental analysis of H_4L ligand and its metal complexes (1-7).

Compounds Mol. formula (M.Wt)	M.P. °c	Color %Yield	(%) found (Calcd.)							Λm*
			C	H	N	Cl	S	P	M	
H_4L $C_{44}H_{42}Cl_4N_{16}O_{12}P_2S_4$ (1319.04)	220	Faint brown (31.75)	39.97 (40.06)	3.19 (3.22)	16.94 (16.99)	10.70 (10.75)	9.68 (9.73)	3.66 (4.70)	–	1.20
(1) $[(Fe)_2(H_4L)Cl_4]Cl_2$ $C_{44}H_{42}Cl_{10}Fe_2N_{16}O_{12}P_2S_4$ (1643.44)	>300	Brown (37.74)	32.09 (32.16)	2.52 (2.58)	13.59 (13.64)	21.50 (21.57)	7.77 (7.81)	3.71 (3.77)	6.74 (6.80)	205.10
(2) $[(Mn)_2(H_4L)Cl_2(H_2O)_2]Cl_2$ $C_{44}H_{46}Cl_8Mn_2N_{16}O_{14}P_2S_4$ (1606.76)	>300	Faint brown (53.77)	32.79 (32.89)	2.82 (2.89)	13.90 (13.95)	17.59 (17.65)	7.92 (7.98)	3.79 (3.85)	6.78 (6.84)	195.40
(3) $[(Co)_2(H_4L)Cl_2(H_2O)_2]Cl_2$ $C_{44}H_{46}Cl_8Co_2N_{16}O_{14}P_2S_4$ (1614.74)	>300	Brown (55.10)	32.68 (32.72)	2.81 (2.88)	13.83 (13.88)	17.49 (17.56)	7.88 (7.94)	3.79 (3.84)	7.25 (7.30)	197.80
(4) $[(Cu)_2(H_4L)Cl_2(H_2O)_2]Cl_2$ $C_{44}H_{46}Cl_8Cu_2N_{16}O_{14}P_2S_4$ (1623.98)	>300	Brown (72.85)	32.48 (32.54)	2.80 (2.86)	13.74 (13.80)	17.40 (17.46)	7.82 (7.90)	3.80 (3.81)	7.77 (7.83)	198.20
(5) $[(Zn)_2(H_4L)Cl_2(H_2O)_2]Cl_2$ $C_{44}H_{46}Cl_8N_{16}O_{14}P_2S_4$ Zn_2 (1627.66)	>300	Yellowish white (65.69)	32.41 (32.47)	2.80 (2.85)	13.68 (13.77)	17.30 (17.42)	7.82 (7.88)	3.78 (3.81)	7.91 (8.04)	194.90
(6) $[(Cd)_2(H_4L)Cl_2(H_2O)_2]Cl_2$ $C_{44}H_{46}Cd_2Cl_8N_{16}O_{14}P_2S_4$ (1721.70)	>300	Faint brown (24.06)	30.62 (30.69)	2.66 (2.70)	12.96 (13.02)	16.40 (16.47)	7.39 (7.45)	3.57 (3.60)	12.75 (13.06)	208.10
(7) $[(UO_2)_2(H_4L)](NO_3)_4$ $C_{44}H_{42}Cl_4N_{20}O_{28}P_2S_4U_2$ (2107.14)	>300	Dark orange (76.93)	24.96 (25.08)	1.95 (2.01)	13.24 (13.30)	6.65 (6.73)	5.96 (6.09)	2.86 (2.94)	–	398.90

* ohm $^{-1}$cm^{2}mol^{-1}

3.4. ^{1}H NMR spectra

The free ligand proton magnetic resonance experiment was carried out in DMSO-d6. Unfortunately, the insolubility of all diamagnetic complexes (5, 6,7) in $CDCl_3$, CD_3COCD_3, or DMSO-d6 makes ^{1}H NMR spectra of these complexes difficult to obtain in order to better understand how the free ligands bond to the metal ions [28] as shown in Fig.1.

3.5. IR spectra and mode of bonding

Infrared spectrum was obtained in the 4000-400 cm-1 region for the free ligand and its metal complexes (1-7). The IR spectra of the complexes were contrasted with those of the free ligand to identify the most probable coordination sites involved in chelation. Chelation was intended to have an impact on the location and/or intensity of these peaks. The sulfonamide group's υ (NH), was discovered at 3422 cm^{-1} or According to a careful examination of the free ligand and its metal complexes, the H_4L ligand was hidden behind the wide bands at 3420–3422 and at 3436–3437 cm^{-1} in the spectrum of the isolated complexes (1–7) for the free ligand. For the H_4L ligand, the sulfone group in the double bond stretching region asym (O=S=O) and sym (O=S=O) were present at 1321and 1090 cm^{-1}. Following interaction with the transition metal ions, these sulfone group bands were relocated to higher frequencies at 1340–1343 cm^{-1} and 1087–1094 cm^{-1} for the ligand H_4L. The red shift of the SO_2 band to

lower frequencies can be attributed to the change of the sulfonamide group (–SO_2NH) to the enol form (–SO(OH)=N) as a result of complex formation to build a more stable six-membered ring [29, 30]. The spectra also indicated a sharp band due to the stretched vibration rings of diazine (C=N), which occurred at 1585 cm^{-1} for the H_4L then changed to 1636–1639 cm^{-1} in the Complexes (1-7) spectra. That shows that the heterocycle ring –N is involved in the production of complexes. The nonligand bands detected at 544–574 cm^{-1} for H_4L metal complexes were attributed to (M–O) of complexes [31]. Coordinating water infrared bands (H_2O) appeared at 829-833 cm^{-1} for metal complexes, indicating water molecule bonding to metal ions [32] as shown in Fig.2 and table 2.

Table 2. IR spectrum bands (cm^{-1}) for H_4L ligand and its metal complexes (1−7).

Comp. No.	υ (NH)/ (OH)	υ(SO_2) (asym.)	υ(SO_2) (sym.)	υ (C=N)	υ (P–N)	υ (P–Cl)	υ(H_2O) (Coord.)	υ(M–O)	υ(M-N)
H_4L	3422sh	1321sh	1090sh	1585sh	1153sh	555sh	–	–	–
(1)	3436br	1342sh	1087m	1639sh	1153sh	595m	829m	574m	420m
(2)	3437m	1342sh	1091sh	1639sh	1149sh	594m	829m	551m	425m
(3)	3436br	1340m	1087br	1639sh	1152sh	595m	831m	544m	428m
(4)	3437m	1343w	1094br	1636sh	1149m	624m	833w	555m	420m
(5)	3437sh	1342sh	1091sh	1639sh	1153sh	594m	829m	547m	429m
(6)	3436sh	1341m	1087sh	1637sh	1151sh	596m	831w	545m	428m
(7)	3437br	1342sh	1088m	1639sh	1153sh	594m	829m	547m	430m

Sh = sharp, m = medium, br = broad, w = weak.

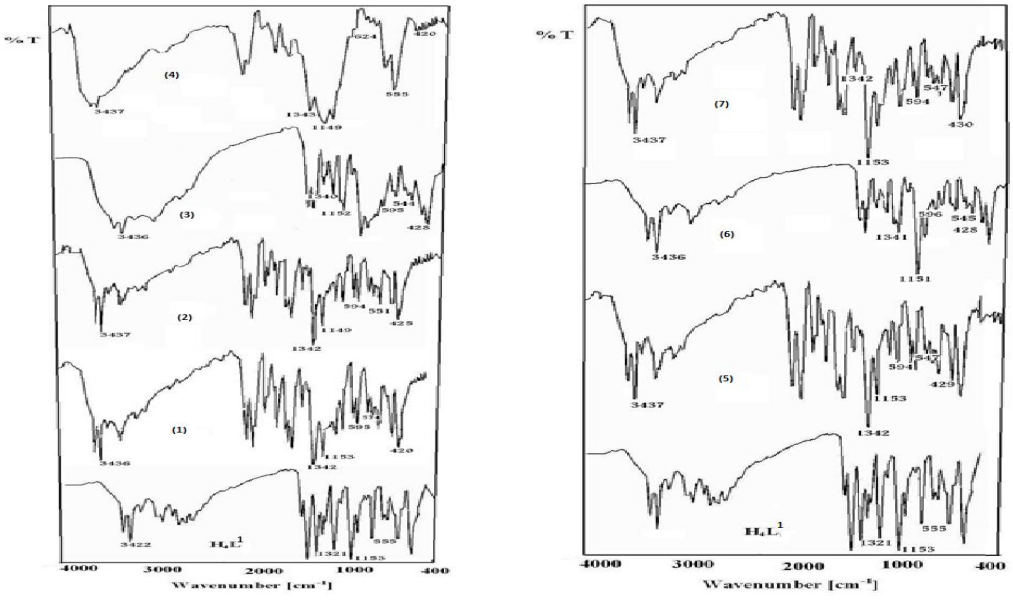

Fig.2. IR spectra of H_4L ligand and its metal complexes.

3.6. Electronic spectra and magnetic properties.

At ambient temperature, DMF has been used to demonstrate the electronic spectra of ligands and also their metal complexes (10^{-3}M) a wavelength region of 200-800 nm.A strong and sharp peak appeared in the UV –vis spectra of the H_4L ligand at 268 nm. This is consistent with the phosphazo four–membered ring [33]. This band undergoes significant shifts to red or blue areas in the spectrum of transition metal complexes upon complexation, depending upon the nature of metal ions coupled to the H_4L ligand. A spectral band that was discovered

for free ligands at 300 nm corresponds to the π-π* transition. Upon complexation, this band shifted as shown in table 3. Fig 3. Furthermore, the complexes' spectra reveal a band mostly in the range of 352–440 nm. which is allocated to the n-π* transition [34]. However, a band discovered at 550–790 nm in the metal complexes was ascribed to all transition metals [35] in table 3.

Also, from the diffuse reflectance spectra of the complexes (1–7), bands of around 23,753 cm^{-1} were revealed in the Fe (III) complex. This might be due to the $^6A_{1g} \rightarrow {}^4T_{2g}(G)$ transition for Fe (III) ions in an octahedral geometry [36,37]. Two bands were also observed at 14,749, 17,301 cm^{-1} which can be credited with $^6A_{1g} \rightarrow {}^4T_{1g}$. The Fe (III) complex's magnetic moment was measured to be just 4.99 B.M, indicating a high spin of an octahedral coordination requiring SP^3d_2 hybridization of Fe^{+3}complex. The spectra additionally display, the 23.753 cm^{-1} band, which might indicate ligand-to-metal charge transfer (L→M) for Fe (III) ion complex [36]. Three bands are evident in the diffuse reflectance spectra of the Mn (II) complex at 15,873, 22,172 and 26,954 cm^{-1} confronted with $^6A_{1g} \rightarrow {}^4T_{1g}$, $^6A_{1g} \rightarrow {}^4T_{2g}(G)$ and $^6A_{1g} \rightarrow {}^4T_{1g}(G)$ transitions, respectively [38,39]. The magnetic moment value is 5.24 B.M., showing the existence of Mn (II) complex in octahedral structures with a high spin [40, 41].

The electronic spectra and magnetic susceptibility of the Co (II) complex are shown in table 4. That confirms an octahedral coordinated high spin [42-45]. The Cu (II) complex solid reflectance demonstrates a broad, low-intensity band located at 17,657 cm^{-1} which may be assigned to $^2T_{2g} \rightarrow {}^2E_g(x^2-y^2)$ transition [46]. Also, the spectra display a band at 23,697 cm^{-1} for Cu (II) ions, referring to (L→M) charge transfer. The Cu^{+2} complex has a magnetic moment of 1.76 B.M., confirming that the structure is octahedral.

All Zn (II), Cd (II) and UO_2 (II) metal complexes have a d^{10} configuration. In the same way as those established for complexes that include O–N donor cyclodiphosphazane–sulfa drug derivatives [47, 48], based on the empirical formula, we suggested an octahedral geometry for these complexes. Table 4.

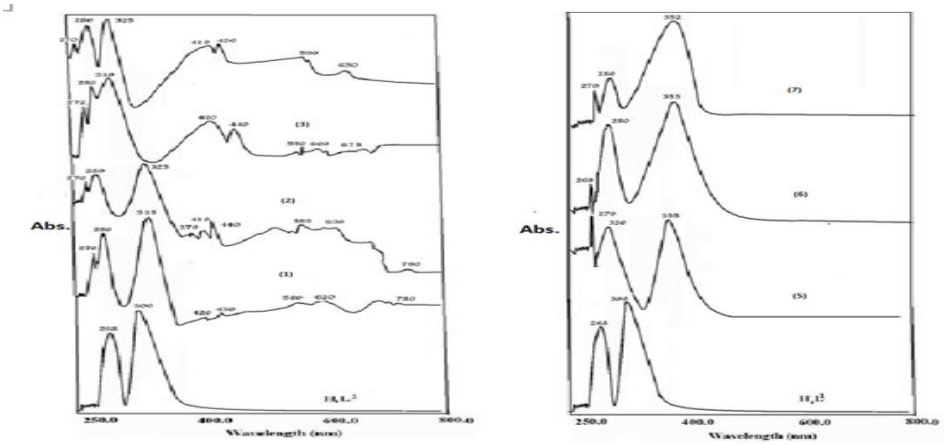

Fig.3. UV–vis spectra for H_4L ligand and its transition metal complexes (1-7).

Table 3 Electronic spectral data of H_4L ligand and its metal complexes (1−7).

Compd. No.	Absorption bands (nm)			
	Phosphazo ring	π-π*	n-π*	*d-d* transition
H_4L	268	300	–	–
(1)	270	280, 315	420, 430	580, 620,780
(2)	270	280, 325	370, 410, 440	585, 630, 790
(3)	272	280, 310	420, 440	550, 600, 675
(4)	270	280, 325	410, 420	590, 630
(5)	270	280, 320	355	–
(6)	269	280	355	–
(7)	270	280	352	–

Table 4. Electronic spectral data and magnetic moment of the ligand and its metal complexes (1−7).

Complex	Geometry	μ_{eff}(B.M.)	Band ssignments	Absorption bands (cm^{-1})
(1)$[(Fe)_2(H_4L^1)Cl_4]Cl_2$	3Octahedral	4.99	$^6A_{1g}\rightarrow{}^4T_{2g}(G)$ $^6A_{1g}\rightarrow{}^4T_{1g}$ LMCT(L→M)	**23,697** **14,005,** **17,241** **23,697**
(2)$[(Mn)_2(H_4L^1)Cl_2(H_2O)_2]Cl_2$	Octahedral	5.24	$^6A_{1g}\rightarrow{}^4T_{1g}$ $^6A_{1g}\rightarrow{}^4T_{2g}(G)$ $^6A_{1g}\rightarrow{}^4T_{1g}(G)$	**15,625** **22,222** **26,455**
(3)$[(Co)_2(H_4L^1)Cl_2(H_2O)_2]Cl_2$	Octahedral	4.12	$^4T_{1g}(F)\rightarrow{}^4A_{2g}(F)$ $^4T_{1g}(F)\rightarrow{}^4T_{2g}(P)$	**17,212** **20,040**
(4)$[(Cu)_2(H_4L^1)Cl_2(H_2O)_2]Cl_2$	Octahedral	1.76	$^2T_{2g}\rightarrow{}^2E_g(x^2-y^2)$ L→M CT	**17,545** **24,449**
(5)$[(Zn)_2(H_4L^1)Cl_2(H_2O)_2]Cl_2$	Octahedral		**d^{10}**	
(6)$[(Cd)_2(H_4L^1)Cl_2(H_2O)_2]Cl_2$	Octahedral		**d^{10}**	
(7)$[(UO_2)_2(H_4L^1)](NO_3)_4$	**Octahedral**		**d^{10}**	

3.7. Powder X-ray diffraction studies

Also, X-ray powder diffraction patterns of the H_4L free ligand and its Cu (II) complex have been obtained. (2θ) for comparison table 5. Fig.4. can be seen for each sample's Bragg angles (2θ), relative intensities (I/Io), and interplanar spacing (d) as well as their peak assignments.

The ligand H_4L and also its Cu (II) complex (4) were investigated using an X-ray diffractogram in the region 0 – 70°(2θ) using Cu Kα as a source. Each diffractor was well resolved into sharp peaks, indicating that the ligand and its complex are extremely crystalline. The crystalline component of the compounds' d-spacing, which is defined as the typical distance between rings in adjacent chains, as well as the interchain distance, were calculated using the Bragg equation. [49]. According to the X-ray diffractogram, the nature of the peaks is well defined, crisp, and of high intensity. Peaks have high intensity, are well-defined, and have high resolution. Under the summits, there was no discernible widening. As a consequence, the ligand as well as its Cu (II) complex obtained from the study crystallized [50].

The ligand's diffraction consists of 50 reflections ranging from 10 to 50° (2), with the maximum reflection at 2 = 43.76°, corresponding to d = 2.01°A. Cu^{+2} complex diffraction consists of 29 reflections ranging from 5 to 65° (2), with the maximum reflection at 2 = 61.17°, which corresponds to d = 1.51°A. [51-53]. Table 5 shows the x-ray diffraction results.

Figure 4 depicts the outcome. The pattern's strong peaks indicate a higher degree of crystallinity. A large unit cell and low symmetry can be inferred because the most intense peak positions were in the low 20 range.

To summarize, the use of metal complexes in drug synthesis is mainly obsolete in pharmaceutical analysis. However, combining these fundamental methodologies with modern instrumental methods for end point signaling, such as infrared and X-ray measurements, opens up new avenues for qualitative analytical application.The data also shows that the Cu (II) complex shares its ligand in the major peaks, with a minor shift and the creation of new peaks, indicating the formation of a new coordination complex compound [54].

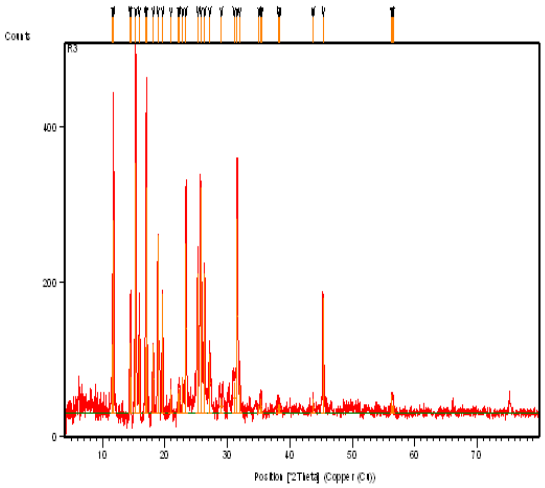

H_4L free ligand.

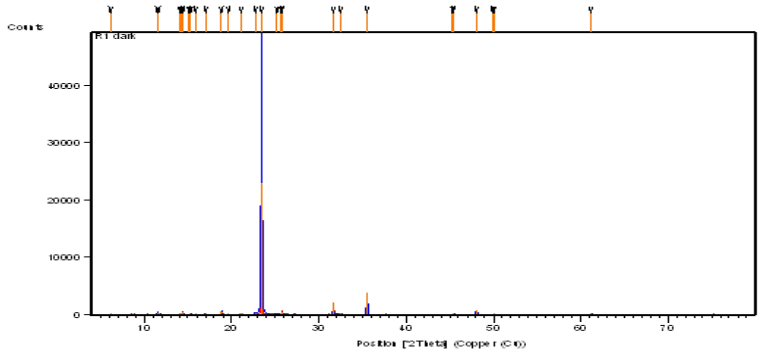

Cu (II) complex of H_4L ligand

Fig.4. X-ray powder diffractogram of H_4L and It's Cu (II) complex.

Table5: X- ray diffraction of H_4L ligand and its Cu complex (4)

	H_4L						(4)		
	d space [A°]	AnglePos. [Ø]	Rel I I/I°	d space [A°]	AnglePos.[Ø]	Rel I I/I°	d space [A°]	AnglePos.[Ø]	Rel I I/I°
1	7.62	11.61	27.75	2.80	31.99	11.65	14.34	6.16	0.26
2	7.62	11.64	13.87	2.80	32.07	5.82	7.69	11.49	0.88
3	7.54	11.73	77.19	2.56	35.10	3.11	7.62	11.60	0.99
4	7.54	11.76	38.60	2.56	35.10	1.56	6.27	14.11	0.21
5	6.14	14.41	28.34	2.54	35.39	6.07	6.21	14.25	0.25
6	6.14	14.45	14.17	2.54	35.48	3.03	6.15	14.40	1.70
7	6.11	14.50	14.32	2.53	35.50	2.14	5.85	15.13	0.08
8	6.11	14.53	7.16	2.53	35.59	1.07	5.81	15.24	0.33
9	5.78	15.31	100.0	2.36	38.14	3.72	5.78	15.31	0.57
10	5.78	15.35	50.00	2.36	38.24	1.86	5.57	15.87	0.65
11	5.57	15.90	31.06	2.34	38.42	3.51	5.21	17.01	0.86
12	5.57	15.92	15.53	2.34	38.52	1.75	4.70	18.85	2.50
13	5.25	16.88	26.80	2.01	43.76	5.93	4.51	19.64	0.36
14	5.25	16.92	13.40				4.21	21.06	0.14
15	5.21	17.01	90.05				3.91	22.72	0.81
16	5.21	17.06	45.02				3.79	23.41	100.0
17	4.89	18.13	27.49				3.79	23.43	88.27
18	4.70	18.89	71.55				3.52	25.22	0.57
19	4.52	19.63	48.16				3.46	25.69	0.69
20	4.24	20.93	10.07				3.45	25.78	1.94
21	4.24	20.99	5.04				2.82	31.63	9.31
22	4.00	22.20	8.15				2.75	32.49	0.72
23	4.00	22.25	4.08				2.52	35.50	17.25
24	3.98	22.33	9.97				1.99	45.32	0.25
25	3.98	22.39	4.98				1.99	45.38	0.75
26	3.88	22.90	14.81				1.89	50.00	2.96
27	3.81	23.34	67.64				0.00	0.00	1.82
28	3.81	23.40	33.82				1.82	50.04	0.48
29	3.53	25.23	56.20				1.51	61.17	0.72
30	3.46	25.71	90.10						
31	3.38	26.34	56.11						
32	3.28	27.19	24.00						
33	3.07	29.05	5.59						
34	2.88	31.08	12.56						
35	2.88	31.16	6.28						
36	2.83	31.58	77.44						
37	2.83	31.66	38.72						

3.8. Thermal analysis

Thermal investigations of the complexes were conducted utilizing the thermogravimetry (TG) technique in the temperature range of 25-900^{o}C for order to improve understanding of the complexes' structure, Fig.5. The predicted mass losses were derived from TG data, whereas the calculated mass losses were based on microanalysis results as shown in table 6.

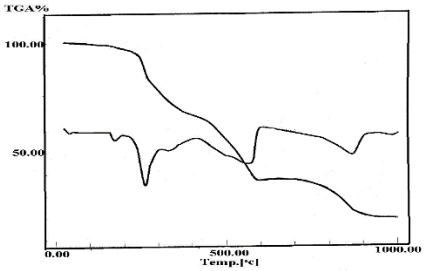

$[(Fe)_2(H_4L^1)Cl_4]Cl_2$,(1).

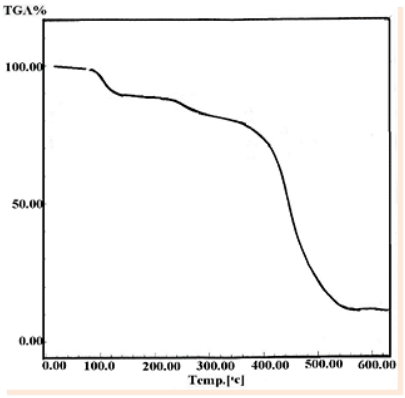

$[(Co)_2(H_4L^1)Cl_2(H_2O)_2]Cl_2$,(3)

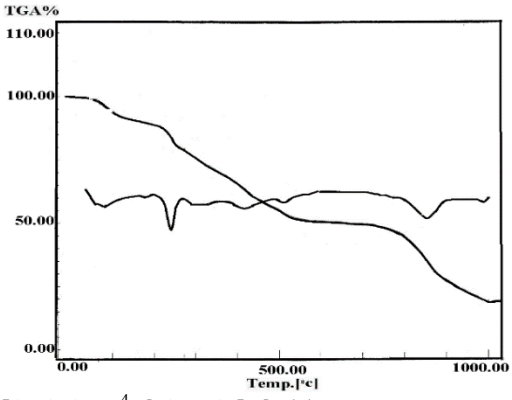

$[(Cu)_2(H_2L^4Cl_2(H_2O)_2]Cl_2$,(5).

Fig.5.TGA curves for Fe (III), Co (II) and Cu (II) complexes (1, 3, 4).

Correlation of all results obtained for the complexes under study gives us information regarding the suggested structure of the complexes to be as in Figs.6

Table 6. Thermogravimetric results (TG) of Fe (III), Co (II) and Cu (II) complexes (1, 3, 4).

Complex	Temp. range (°C)	n*	Loss in weight Estim./(calcd.)%		Loss in weight Estim. / (calcd.)%	Metallic residue
			Mass loss	Total mass loss		
(1) $[(Fe)_2(H_4L)Cl_4]Cl_2$	180-220 220-420 420-610 610-900	4	4.50(4.69) 30.75(30.52) 28.83(28.78) 15.13(15.17)	79.21(79.16)	-Loss of 2HCl -Loss of 2HCl and $C_{13}H_{10}N_6O_6S$ -Loss of $C_{28}H_{14}N_6P_2$, SO_2 and O_2 -Loss of $C_{11}H_{12}N_2$ and S_2 leaving $C_2H_4N_2P_2$	Fe_2O_3
(3) $[(Co)_2(H_4L)Cl_2(H_2O)_2]Cl_2$	70-100 100-272 272-424 599-424 599-790	5	9.92 (9.52) 6.93(6.91) 8.15(8.51) 6.00(6.55) 51.06(51.50)	84.60(82.95)	-Loss of $2H_2O$ Coord. and 3HCl -Loss of $C_6H_{10}Cl$ -Loss of $C_6H_{12}NO_2$ -Loss of $C_5H_{10}NO$ -Loss of $C_{25}H_{32}N_{12}O_9P_2S_4$	$2CoCl_2$
(4) $[(Cu)_2(H_4L)Cl_2(H_2O)_2]Cl_2$	80-200 200-280 280-780 780-880 880-10	5	4.69(4.71) 4.07(4.75) 12.84(12.73) 11.23(11.91) 48.22(48.41)	81.05(82.51)	-Loss of $2H_2O$ Coord. and HCl -Loss of 2HCl -Loss of of HCl and $C_{11}H_{11}O$ -Loss of C_6H_5N, N_2 and SO_2 -Loss of $C_{25}H_{20}N_{11}O_7P_2S_3$	$2CuCl_2$

n* = number of decomposition steps.

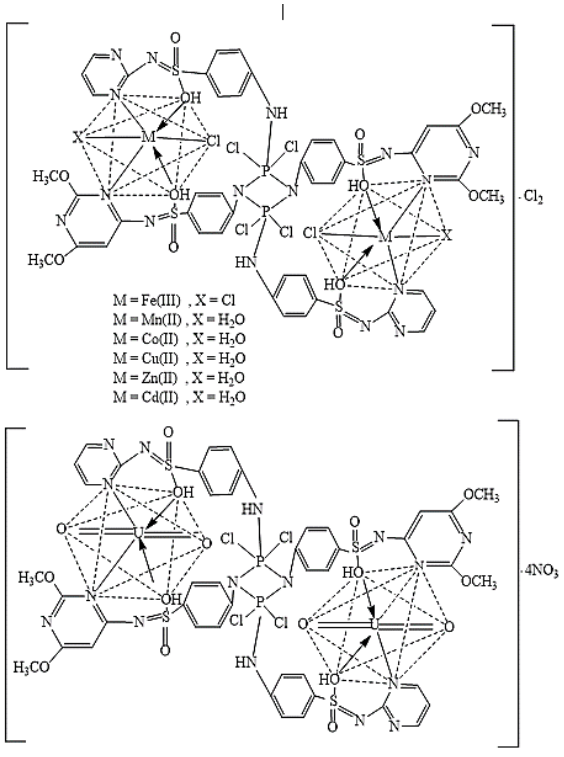

Fig.6. suggested structure of the newly obtained H_4L free ligand metal complexes (1−7).

3.9. Antimicrobial activity

The fundamental purpose of any antibacterial chemical's development and manufacturing is to inhibit harmful microorganisms without creating any side effects on the patients. We employed more than one test organism in the antimicrobial screening of

the newly the newly synthesized compounds, free ligand with its metal complexes, to boost the chances of detecting the antibiotic potential of the tested materials (1–7). The sensitivity of a microorganism to antibiotics and other antimicrobial treatments was assessed using test plates. Tables 7 & Figs.7-8 which were cultivated at 28°C for 2 days (fungi) and 37°C for 1 day (bacteria) (for bacteria).

Staphylococcus aureus, Micrococcus sp, and Staphylococcus epidemidis as Gram–positive bacteria, Escherichia coli, Pseudomonas aeruginosa, Acinetobacter species, Proteus mirabilis, and Klebsiella pneumoniae as Gram–negative bacteria were screened with the parent free ligand and its metal complexes (100 g/l in DMF as a solvent). Antifungal activity against Candida species was also investigated. Using agar nutrition as a medium, the antibiotic Chloramphenicol was employed as a standard antibacterial control and Cefotaxime was utilized as a standard antifungal control. For the set of assays, a solvent control using DMF was performed. When the inhibitory effects of the parent free ligand were compared, it was discovered that the parent free ligand had a remarkable antimicrobial activity against all tested species (Gram–positive, Gram–negative bacteria, and fungi), had a greater inhibitory effect on the growth of different tested strains, and the results are shown in Tables 7, and Figs. 7–8.

On replacement of two chlorine atoms in H_2L free ligand with two molecules of mono silver sulfadiazine molecules to create H_4L, the antibacterial activity of this free ligand enhanced to a larger extent than the original H_2L free ligand against all bacterial and fungal strains examined. [53]. the antimicrobial activities of the ligand and all complexes showed a remarkable activity against all bacterial and fungal strains. Among the prepared complexes (1-7)

(a)

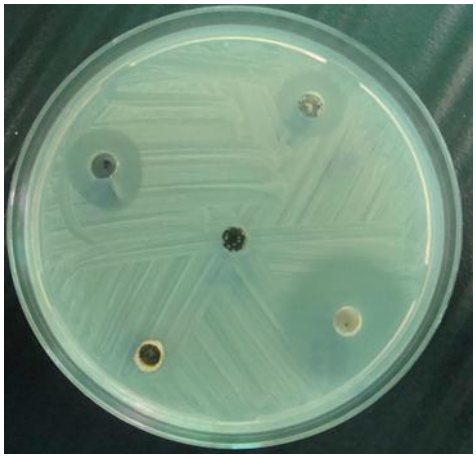

(b)

Fig.7.Photograph showing antibacterial screening of:

(a) H_4L free ligand and its metal complexes Fe (III), Mn (II), Zn (II) and Cd (II) against Pseudomonas aeruginosa.

(b) H_4L free ligand and its metal complexes Fe (III), Mn (II), Zn (II) and Cd (II) against Candida sp.

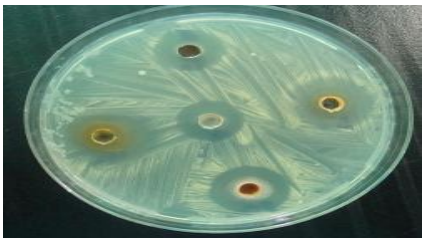

(c)

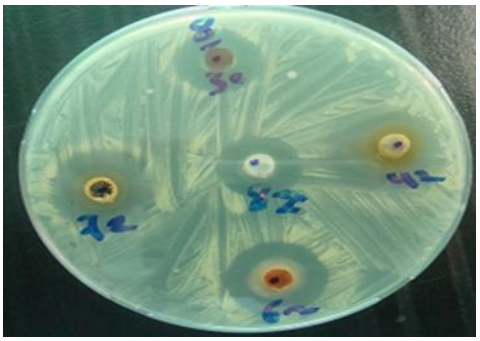

(d)

Fig.8. Photograph showing antibacterial screening of:

(c) H_4L free ligand and its metal complexes Fe (III), Mn (II), Zn (II) and Cd (II) against Escherichia coil

(d) H_4L free ligand and its metal complexes Fe (III), Cu (II), Zn (II) and Cd (II) against (staphylocos aureus)

Table 7. Antimicrobial activity of H4L free ligand and its metal complexes (1−7) *.

Fungi	Candida sp	14	20	18	11	12	19	16	9	0
Gram-negative bacteria	Klebsiella pneumoniae	10	15	13	11	15	14	13	11	0
	Proteus mirabilis	10	15	12	9	13	13	14	10	0
	Acinetobacter sp	11	20	17	11	15	15	17	13	0
	Pseudomonas aeruginosa	18	19	17	14	16	20	18	15	0
	Escherichia coli	22	24	21	10	15	25	20	12	25
Gram-positive bacteria	Staphylocous epidemidis	12	15	13	12	13	15	14	11	0
	Micrococcus sp	17	18	14	15	15	19	18	12	39
	Staphylocos aureus	15	16	16	13	15	19	18	12	30
Compound No.		**H_4L**	**(1)$[(Fe)_2(H_2L)Cl_4]Cl_2$**	**(2)$[(Mn)_2(H_2L)Cl_2(H_2O)_2$**	**(3) $[(Co)_2(H_2L)Cl_2(H_2O)_2]Cl_2$**	**(4) $[(Cu)_2(H_2L)Cl_2(H_2O)_2]Cl_2$**	**(5) $[(Zn)_2(H_2L)Cl_2(H_2O)_2]Cl_2$**	**(6) $[(Cd)_2(H_2L)Cl_2(H_2O)_2]Cl_2$**	**(7) $[(UO_2)_2(H_2L)](NO_3)_4$**	**R.S. ****

*The test done using the diffusion agar technique. Inhibition values 1-5 mm beyond control = (less active). Inhibition values 6-10 mm beyond control = (moderate active). Inhibition values 11-15 mm beyond control = (highly active). Inhibition values over 15 mm beyond control = (very highly active). Not active = 0.

**The antibiotic Chloramphenicol was used as standard antibacterial control and Cefotaxime was used as standard antifungal control.

3.10. Potential cytotoxicity measurement

Human cancer cell lines (HCT116) were used to test the synthesized compounds' anticancer potential in vitro. Colorectal cancer, commonly known as bowel cancer, is the third most frequent type of cancer. The connection between drug concentrations and cell viability was also plotted to compute the IC50 (the concentration required to inhibit cell viability by (50%),) and the results were provided in Tables 8.

All of the examined compounds demonstrated greater inhibitory action against colon carcinoma cell line in the anticancer screening test for H_4L free ligand and its metal complexes. While $[(Mn)_2(H_4L)Cl_2(H_2O)_2]Cl_2$ had a higher inhibitory activity (65%) than its free ligand H_4L (45%) and the other complexes examined.

Finally, the order of the effectiveness of all these tested compounds was recorded as:

Mn (II) > Cu (II) > Zn (II) > UO_2 (II) > Cd (II) > Co (II) > H_4L > Fe (III).

Table 8. The antitumor properties of H_4L ligand and its metal complexes (1− 7).

HCT116	
Sample	Inhibition %
H_4L	**45**
(1)$[(Fe)_2(H_4L^1)Cl_4]Cl_2$	**23**
(2)$[(Mn)_2(H_4L^1)Cl_2(H_2O)_2$	**65**
(3) $[(Co)_2(H_4L^1)Cl_2(H_2O)_2]Cl_2$	**50**
(4) $[(Cu)_2(H_4L^1)Cl_2(H_2O)_2]Cl_2$	**62**
(5) $[(Zn)_2(H_4L^1)Cl_2(H_2O)_2]Cl_2$	**58**
(6) $[(Cd)_2(H_4L^1)Cl_2(H_2O)_2]Cl_2$	**53**
(7) $[(UO_2)_2(H_4L^1)](NO_3)_4$	**54**

4.Conclusion:

In this research, symmetrically cyclodiphosphazane ligands and numerous metal complexes were synthesized and examined using a variety of physicochemical methods. The antibacterial and anticancer properties of the ligands and their metal complexes have been investigated. The ligands and their complexes were discovered to have very high to high antibacterial activity against a variety of bacteria and fungi, as well as anticancer efficacy against colon carcinoma HCT116.

References

1. Chaptal, C. J. D. (2021). Elements of Chemistry. By M. I. A. Chaptal. Translated From the French. (2nd Ed.); Vol. 1. Legare Street Press.
2. Sydam, R., & Deepa, M. (2013). A new organo-inorganic hybrid of poly(cyclotriphosphazene-4,4′-bipyridinium) chloride with a large electrochromic contrast. Journal of Materials Chemistry C, 1(47), 7930. https://doi.org/10.1039/c3tc31486c

3. Kharissova, O., Méndez-Rojas, M., Kharisov, B., Méndez, U., & Martínez, P. (2014). Metal Complexes Containing Natural and Artificial Radioactive Elements and Their Applications. Molecules, 19(8), 10755–10802. https://doi.org/10.3390/molecules190810755
4. Sharaby, C. M., Amine, M. F., & Hamed, A. A. (2017). Synthesis, structure characterization and biological activity of selected metal complexes of sulfonamide Schiff base as a primary ligand and some mixed ligand complexes with glycine as a secondary ligand. Journal of Molecular Structure, 1134, 208–216. https://doi.org/10.1016/j.molstruc.2016.12.070
5. El-Wahab, H. A., El-Fattah, M. A., El-Khalik, N. A., & Sharaby, C. M. (2012). Synthesis and performance of flame retardant additives based on cyclodiphosph(V)azane of sulfaguanidine,1,3-di-[N/-2-pyrimidinylsulfanilamide]-2, 2, 2.4, 4, 4-hexachlorocyclodiphosph(V)azane and 1,3-di-[N/-2-pyrimidinylsulfanilamide]-2, 4-di[aminoacetic acid]-2, 4-dichlorocyclodiphosph(V)azane incorporated into polyurethane varnish. Progress in Organic Coatings, 74(3), 615–621. https://doi.org/10.1016/j.porgcoat.2012.02.010
6. Khan, F., Syed, F., Iqbal, A., Khan, Z. U. H., Ullah, H., & Khan, S. (2016). Synthesis, Spectral Characterization and Antibacterial Study of Schiff Base Metal Complexes Derived from 4-Bromo-N-[(E)-(5-chloro-2-hydroxyphenyl)methylidene]benzenesulfonamide . Asian Journal of Chemistry, 28(8), 1658–1660. https://doi.org/10.14233/ajchem.2016.19771
7. Nakahata, D. H., de Paiva, R. E. F., Lustri, W. R., & Corbi, P. P. (2020). Sulfonamide-containing copper(ii) complexes: new insights on biophysical interactions and antibacterial activities. New Journal of Chemistry, 44(40), 17236–17244. https://doi.org/10.1039/d0nj01889a
8. Pandey, M. K., Kunchur, H. S., Ananthnag, G. S., Mague, J. T., & Balakrishna, M. S. (2019). Catechol and 1,2,4,5-tetrahydroxybenzene functionalized cyclodiphosphazane ligands: synthesis, structural studies, and transition metal complexes. Dalton Transactions, 48(11), 3610–3624. https://doi.org/10.1039/c8dt04819c
9. Abeer T. Abdelkarim, (2015) Spectroscopic characterization of novel Cu (II) mixed ligand complexes involving tridentate hydrazone ligand and some amino acids as antibacterial and antioxidant agents, Int. J. Pharma Sci., 5 839 - 851.
10. Vogel, A., I. (2022). A Text-Book of Quantitative Inorganic Analysis - Theory and Practice Second Edition. Longmans, Green and Co.
11. Marek J, Farmakoterapie vnitrnich nemoci (Pharmacotherapy of Internal Diseases), Grada Publishing, Prague, 1998, p. 159.
12. Msagati T.A.M, Nindi M.M, (2004).Multiresidue determination of sulfonamides in a variety of biological matrices by supported liquid membrane with high pressure liquid chromatographyelectrospray mass spectrometry detection. Talanta 64, 87–100.
13. Zhmurova,I.N. and Kirsanov,A.V., Zh. Obshch. Khim. 32 (1962), 2576−80 Chem.Abst. 58, (1963), 7848e.
14. Schwarzenbach, G. (1969). Complexometric titrations (2nd ed.). Methuen.
15. Voy,R., Chem., ZIg.Chem., Apparatus, (1897), 21, 941
16. Kitzberger, C. S. G., Smânia, A., Pedrosa, R. C., & Ferreira, S. R. S. (2007). Antioxidant and antimicrobial activities of shiitake (Lentinula edodes) extracts obtained by organic solvents and supercritical fluids. Journal of Food Engineering, 80(2), 631–638. https://doi.org/10.1016/j.jfoodeng.2006.06.013
17. Skehan, P., Storeng, R., Scudiero, D., Monks, A., McMahon, J., Vistica, D., Warren, J. T., Bokesch, H., Kenney, S., & Boyd, M. R. (1990). New Colorimetric Cytotoxicity Assay for Anticancer-Drug Screening. JNCI Journal of the National Cancer Institute, 82(13), 1107–1112. https://doi.org/10.1093/jnci/82.13.1107
18. Mallikarjun, G. (2017). Synthesis, Characterization and Biological Activity of Schiff Base Metal Complexes. Asian Journal of Research in Chemistry, 10(4), 587. https://doi.org/10.5958/0974-4150.2017.00098.0
19. Abd-ellah, I. M., Al-shaibi, Y., Ba-issa, A. A., & El-hammadi, M. S. (1998). SPECTROSCOPIC STUDY ON THE ELECTRON DELOCALIZATION WITHIN THE PHOSPHAZO RING. Phosphorus, Sulfur, and Silicon and the Related Elements, 139(1), 29–43. https://doi.org/10.1080/10426509808035675

20. Mahmoud, W. H., Mohamed, G. G., & El-Sayed, O. Y. (2017). Coordination compounds of some transition metal ions with new Schiff base ligand derived from dibenzoyl methane. Structural characterization, thermal behavior, molecular structure, antimicrobial, anticancer activity and molecular docking studies. Applied Organometallic Chemistry, 32(2). https://doi.org/10.1002/aoc.4051
21. Khalil, M. M. H., Ismail, E. H., Mohamed, G. G., Zayed, E. M., & Badr, A. (2012). Synthesis and characterization of a novel schiff base metal complexes and their application in determination of iron in different types of natural water. Open Journal of Inorganic Chemistry, 02(02), 13–21. https://doi.org/10.4236/ojic.2012.22003
22. Taha, R. H., El-Shafiey, Z. A., Salman, A. A., El-Fakharany, E. M., & Mansour, M. M. (2019). Synthesis and characterization of newly synthesized Schiff base ligand and its metal complexes as potent anticancer. Journal of Molecular Structure, 1181, 536–545. https://doi.org/10.1016/j.molstruc.2018.12.055
23. Mohamed, G. G., & Sharaby, C. M. (2007). Metal complexes of Schiff base derived from sulphametrole and o-vanilin. Spectrochimica Acta Part A: Molecular and Biomolecular Spectroscopy, 66(4–5), 949–958. https://doi.org/10.1016/j.saa.2006.04.033
24. Alaghaz, A. N. M., Ammar, Y. A., Bayoumi, H. A., & Aldhlmani, S. A. (2014). Synthesis, spectral characterization, thermal analysis, molecular modeling and antimicrobial activity of new potentially N2O2 azo-dye Schiff base complexes. Journal of Molecular Structure, 1074, 359–375. https://doi.org/10.1016/j.molstruc.2014.05.078
25. Deilami, A. B., Salehi, M., Arab, A., & Amiri, A. (2018). Synthesis, crystal structure, electrochemical properties and DFT calculations of three new Zn(II), Ni(II) and Co(III) complexes based on 5-bromo-2-((allylimino)methyl)phenol Schiff-based ligand. Inorganica Chimica Acta, 476, 93–100. https://doi.org/10.1016/j.ica.2018.02.013
26. Anacona, J., & Pineda, Y. (2016). Synthesis, Characterization and Antibacterial Activity of a Tridentate Schiff Base Derived from Cephalexin and 1,6-Hexanediamine and its Transition Metal Complexes. Medicinal Chemistry, 6 (7). https://doi.org/10.4172/2161-0444.1000385.
27. Imran, M., Iqbal, J., Iqbal, S. and Ijaz, N., (2007). In Vitro Antibacterial Studies of Ciprofloxacin-Imines and Their Complexes with Cu (II), Ni (II), Co (II), and Zn (II). Turkjsh Journal of Biology, 31,67-72.
28. Panda, J., Das, S., Patnaik, A. K., & Padhi, S. (2020). Interaction of Metal (II) Ion–Ciprofloxacin–Glycine in Solution. Journal of Pharmaceutical Innovation, 16 (3), 454–468. https://doi.org/10.1007/s12247-020-09451-3
29. Mishra,A.; Sharma,R. and Shrivastava,B.D.,(2011).Spectroscopic studies on transition metal iron complexes of 2-(N- Aryietanimidoyl) phenol as ligands, Indian J. Pure and Applied Physics, 49, 740−747.
30. Shama Sh., Sharma N., Jain B. and Malik S., (2014) .Complexation of Ni and VO metals with bidentate schiff base derived from Sulfamethoxazole drug, Derchemica Sinica, 5(5), , 61-66. ISSN: 0976-8505
31. Ramadan, A. M., Bayoumi, H. A., & Elsamra, R. M. I. (2021). Synthesis, characterization, biological evaluation, and molecular docking approach of nickel (II) complexes containing O, N-donor chelation pattern of sulfonamide-based Schiff bases. Applied Organometallic Chemistry, 35 (12). https://doi.org/10.1002/aoc.6412
32. Azam, F., Singh, S., Khokhra, S. L., & Prakash, O. (2007). Synthesis of Schiff bases of naphtha[1,2-d]thiazol-2-amine and metal complexes of 2-(2′-hydroxy)benzylideneaminonaphthothiazole as potential antimicrobial agents. Journal of Zhejiang University SCIENCE B, 8(6), 446–452. https://doi.org/10.1631/jzus.2007.b0446
33. Mohamed, G. G., Zayed, M., & Abdallah, S. (2010). Metal complexes of a novel Schiff base derived from sulphametrole and varelaldehyde. Synthesis, spectral, thermal characterization and biological activity. Journal of Molecular Structure, 979(1–3), 62–71. https://doi.org/10.1016/j.molstruc.2010.06.002
34.) Mohamed,G.G.; Omar,M.M. and Hindy,A.M., (2006) .Metal complexes of Schiff bases. Preparation, characterization and biological activity, Turkish J. Chem., 30, 361-382.
35. Zayed, M., Nour El-Dien, F., Mohamed, G. G., & El-Gamel, N. E. (2004). Structure investigation, spectral, thermal, X-ray and mass characterization of piroxicam and its metal complexes. Spectrochimica Acta Part A: Molecular and

Biomolecular Spectroscopy, 60(12), 2843–2852. https://doi.org/10.1016/j.saa.2003.12.051

36. Soliman, A., & Linert, W. (1999). Investigations on new transition metal chelates of the 3-methoxy-salicylidene-2-aminothiophenol Schiff base. Thermochimica Acta, 338(1–2), 67–75. https://doi.org/10.1016/s0040-6031(99)00201-4
37. Mondal, N., Dey, D. K., Mitra , S., & Malik , K. (2000). Synthesis and structural characterization of mixed ligand η1-2-hydroxyacetophenone complexes of cobalt (III). Polyhedron, 19(28), 2707–2711. https://doi.org/10.1016/s0277-5387(00)00584-2
38. Kohout, J., Hvastijová, M., KožíšEk, J., Garcia DíAz, J., Valko, M., Jäger, L., & Svoboda, I. (1999). Cyanamidonitrate–copper(II) complexes of imidazole ligands: X-ray crystallography and physical investigation. Inorganica Chimica Acta, 287(2), 186–192. https://doi.org/10.1016/s0020-1693(99)00013-4
39. Shilpa, K. G., Shivaprasad, K. H., & Archana, R. (2021). Synthesis, characterization, antimicrobial and Anti-inflammatory study of some novel Schiff bases metal complexes derived from the drug, Diclofenac. Rasayan Journal of Chemistry, 14(04). https://doi.org/10.31788/rjc.2021.1446507
40. Podorov, S. G., Faleev, N. N., Pavlov, K. M., Paganin, D. M., Stepanov, S. A., & Förster, E. (2006). A new approach to wide-angle dynamical X-ray diffraction by deformed crystals. Journal of Applied Crystallography, 39(5), 652–655. https://doi.org/10.1107/s0021889806025696
41. Kumar, L. V., & Nath, G. R. (2019). Synthesis, characterization and biological studies of cobalt (II), nickel (II), copper (II) and zinc (II) complexes of vanillin-4-methyl-4-phenyl-3-thiosemicarbazone. Journal of Chemical Sciences, 131(8). https://doi.org/10.1007/s12039-019-1658-x.
42. S., C., & G., C. (2014). Synthesis, characterization and thermal analysis of the copper(II) complexes with 2,2-bipyridyl and 1,10-phenanthroline. African Journal of Pure and Applied Chemistry, 8(10), 162–175. https://doi.org/10.5897/ajpac2014.0592
43. Dholakiya, P. P., & Patel, M. N. (2004). Metal Complexes: Preparation, Magnetic, Spectral, and Biocidal Studies of Some Mixed-Ligand Complexes with Schiff Bases Containing NO and NN Donor Atoms. Synthesis and Reactivity in Inorganic and Metal-Organic Chemistry, 34(3), 553–563. https://doi.org/10.1081/sim-120030440
44. Patil, R., Delekar, S., Mane, D., & Hankare, P. (2013). Synthesis, structural and magnetic properties of different metal ion substituted nanocrystalline zinc ferrite. Results in Physics, 3, 129–133. https://doi.org/10.1016/j.rinp.2013.08.002
45. Fabbiani, F. P. A., Byrne, L. T., McKinnon, J. J., & Spackman, M. A. (2007). Solvent inclusion in the structural voids of form II carbamazepine: single-crystal X-ray diffraction, NMR spectroscopy and Hirshfeld surface analysis. CrystEngComm, 9(9), 728. https://doi.org/10.1039/b708303n
46. Ebsworth, E. A. V., Lewis, J., Burgess, J., Downs, A. J., Turner, J. J., Mabbs, F. E., Machin, D. J., & Kohl, F. J. (1966). Inorganic chemistry. Annual Reports on the Progress of Chemistry, 63, 129. https://doi.org/10.1039/ar9666300129
47, Raman, N., Johnson Raja, S., & Sakthivel, A. (2009). Transition metal complexes with Schiff-base ligands: 4-aminoantipyrine based derivatives–a review. Journal of Coordination Chemistry, 62(5), 691–709. https://doi.org/10.1080/00958970802326179

48. Rania H. Taha, Preparation, (2015).Spectroscopic Characterization, DNA Cleavage, Antimicrobial and Antitumor Investigations of Nickel and Uranyl Schiff Base Complexes in Bulk and Nano size, Current Science International, 4(4), 684-700. ISSN: 2077-4435.

48. S.Rangaswamy, A. K. M. R. S. (2015). Synthesis, Characterization, Antimicrobial Activity, Antifungal Activity and DNA Cleavage Studies of Transition Metal Complexes with Schiff Base Ligand. International Journal of Innovative Research in Science, Engineering and Technology, 04(02), 60–66. https://doi.org/10.15680/ijirset.2015.0402010

49. Murugesan, R., & Subramanian, E. (2002). Metal oxalate complexes as novel inorganic dopants: Studies on their effect on conducting polyaniline. Bulletin of Materials Science, 25(7), 613–618. https://doi.org/10.1007/bf02707894

50. Patill,A.R.; Donde,K.J.; Raut1,S.S.; Patil,V.R. and Lokh- ande,R.S., J.), (2012), Synthesis, characterization and biological activity of mixed ligand Co (II) complexes of schiff base 2-amino-4-nitrophenol-n-salicylidene with some amino acids, Chemical and Pharmaceutical Research, 4(2)1413−1425.
51. Gavali,L.V. and Hankarep,P.P., (2007), Synthesis and Characterization of the Complexes of Some Transition Metals with 4-[2'-hydroxy salicylidene-5(2-thiazolyazo] Chlorobenzene, J. Physical Sciences, 11, 147−155.
52. P. Mishra, A., Tiwari, A., & K. Jain, R. (2012). Microwave Induced Synthesis And Characterization Of Semiconducting 2-thiophenecarboxaldehyde Metal Complexes. Advanced Materials Letters, 3(3), 213–219. https://doi.org/10.5185/amlett.2011.9307
53. Aly, H. M., Taha, R. H., El-deeb, N. M., & Alshehri, A. (2018). Efficient procedure with new fused pyrimidinone derivatives, Schiff base ligand and its La and Gd complexes by green chemistry. Inorganic Chemistry Frontiers, 5(2), 454–473. https://doi.org/10.1039/c7qi00694b
54. Mohamed El-Sakhawy, Hassan M . Awad, Hassan M.F.Madkour Ahmed K.El-
Ziaty,Mona Abdelkader Nassar, and Salah A.A. Moamed; Preparation and application of organophosphorus dimers as antimicrobial agents for bagasse packaging paper. Cellulose Chem. Technol.,52,(7-8),(2018),655-62.